Atmos. Chem. Phys. Discuss., 15, 12213–12240, 2015
www.atmos-chem-phys-discuss.net/15/12213/2015/
doi:10.5194/acpd-15-12213-2015

Atmospheric Chemistry and Physics Discussions

An algorithm for the numerical solution of the multivariate master equation for stochastic coalescence

L. Alfonso

Universidad Autónoma de la Ciudad de México, México City, 09790, México

Received: 27 February 2015 – Accepted: 23 March 2015 – Published: 23 April 2015

Correspondence to: L. Alfonso (lesterson@yahoo.com)

Published by Copernicus Publications on behalf of the European Geosciences Union.

Abstract

In cloud modeling studies, the time evolution of droplet size distributions due to collision-coalescence events is usually modeled with the kinetic collection equation (KCE) or Smoluchowski coagulation equation. However, the KCE is a deterministic equation with no stochastic fluctuations or correlations. Therefore, the full stochastic description of cloud droplet growth in a coalescing system must be obtained from the solution of the multivariate master equation, which models the evolution of the state vector for the number of droplets of a given mass. Unfortunately, due to its complexity, only limited results were obtained for certain type of kernels and monodisperse initial conditions. In this work, a novel numerical algorithm for the solution of the multivariate master equation for stochastic coalescence that works for any type of kernels, multivariate initial conditions and small system sizes is introduced. The performance of the method was checked by comparing the numerically calculated particle mass spectrum with analytical solutions of the master equation obtained for the constant and sum kernels. Correlation coefficients were calculated for the turbulent hydrodynamic kernel, and true stochastic averages were compared with numerical solutions of the kinetic collection equation for that case. The results for collection kernels depending on droplet mass demonstrates that the magnitude of correlations are significant, and must be taken into account when modeling the evolution of a finite volume coalescing system.

1 Introduction

The evolution of the size distribution of coalescing particles has often been described by the kinetic collection (hereafter KCE) or Smoluchowski coagulation equation, known under a number of names ("stochastic collection", "coalescence"). The discrete form of this equation has the form (Pruppacher and Klett, 1997):

ACPD
15, 12213–12240, 2015

$$\frac{\partial N(i,t)}{\partial t} = \frac{1}{2}\sum_{j=1}^{i-1} K(i-j,j)N(i-j)N(j) - N(i)\sum_{j=1}^{\infty} K(i,j)N(j) \quad (1)$$

where $N(i,t)$ is the average number of droplets with mass x_i, and $K(i,j)$ is the collection kernel related to the probability of coalescence of two droplets of masses x_i and x_j. In Eq. (1), the time rate of change of the average number of droplets with mass x_i is determined as the difference between two terms: the first term describes the average rate of production of droplets of mass x_i due to coalescence between pairs of drops whose masses add up to mass x_i, and the second term describes the average rate of depletion of droplets with mass x_i due to their collisions and coalescence with other droplets.

Within the kinetic approach (Eq. 1), it is assumed that fluctuations are negligible small. This assumption can only be correct if the volume and the number of particles are infinite large. An alternative approach considers the coalescence process in a system of finite number of particles, with fluctuations that are no longer negligible. This finite-volume description is intrinsically stochastic and has been pioneered by Marcus (1968), Bayewitz et al. (1974) and studied in detailed by Lushnikov (1978, 2004) and Tanaka and Nakazawa (1993).

Within the finite volume description a system of particles whose total mass is M_T is considered. The mass distribution of the particles is described by giving the number n_i of particles with mass i, i.e. n_1, n_2, n_3, ..., n_N. Then, the state of the mass distribution of the particle system is described by the N dimensional state vector $\overline{n} = (n_1, n_2, \ldots, n_N)$. The time evolution of the joint probability $P(n_1, n_2, \ldots, n_N; t)$ that the system is in state $\overline{n} = (n_1, n_2, \ldots, n_N)$ at time t is calculated according to the equation (Tanaka and Nakazawa, 1993):

ACPD
15, 12213–12240, 2015

$$\frac{\partial P(\overline{n})}{\partial t} = \sum_{i=1}^{N}\sum_{j=i+1}^{N} K(i,j)(n_i+1)(n_j+1)P(\ldots,n_i+1,\ldots,n_j+1,\ldots,n_{i+j}-1,\ldots;t)$$
$$+ \sum_{i=1}^{N}\frac{1}{2}K(i,i)(n_i+2)(n_i+1)P(\ldots,n_i+2,\ldots,n_{2i}-1,\ldots;t)$$
$$- \sum_{i=1}^{N}\sum_{j=i+1}^{N} K(i,j)n_i n_j P(\overline{n};t) - \sum_{i=1}^{N}\frac{1}{2}K(i,i)n_i(n_i-1)P(\overline{n};t) \quad (2)$$

The master Eq. (2) is a gain-loss equation for the probability of each state $\overline{n} = (n_1, n_2, \ldots, n_N)$. The sum of the first two terms is the gain due to transition from other states, and the sum of the last two terms is the loss due to transitions into other states. The gain terms show that the system may be reached from any state with an i-mer and a j-mer more, and one $(i+j)$-mer less. In Eq. (2) $K(i,j)$ is the collection kernel and the transition rates are $K(i,j)(n_i+1)(n_j+1)$ if $i \neq j$ and $K(i,i)(n_i+1)(n_i+2)$ if $i = j$. From conservation of the total probability, $P(\overline{n};t)$ must satisfy the relation:

$$\sum_{\overline{n}} P(\overline{n};t) = 1 \quad (3)$$

where the sum is taken over all states. Moreover, the total mass M_T of the system must be conserved, and the particle number n_i should be non-negative for any mass x_i:

$$\sum_{i=1}^{N} x_i n_i = M_T, \quad n_i \geq 0, \quad i = 1,\ldots,N \quad (4)$$

Exact solutions of Eq. (2) are only known for a limited number of cases (constant, sum and product kernels) and for monodisperse initial conditions. For these special

ACPD
15, 12213–12240, 2015

cases the master equation has been solved by Lushnikov (1978, 2004) and Tanaka and Nakazawa (1993) in terms of the generating function of $P(\overline{n};t)$. For general, multidisperse initial conditions, the solution of Eq. (2) is not known.

Additionally, for stochastic coagulation, approximate solutions were calculated by using the Van Kampen's system size expansion or Ω-expansion (Van Dongen and Ernst, 1987; Van Dongen, 1987) which permits to find solutions of Eq. (2) valid in the limit of a large system. However, the system size expansion gives less reliable results when applied to systems with a low number of particles or small volumes.

Then, in order to obtain solutions for more realistic kernels (Brownian motion, differential sedimentation etc.), a small number of particles and general multidisperse initial conditions, it has to be solved numerically. In this paper, we present an algorithm that can be applied to obtain the solution of Eq. (2) for any type of kernels and initial conditions. By applying this method, numerical solutions of the master equation were obtained for realistic kernels relevant to cloud physics, along with calculation of the correlations for the number of droplets for different sizes.

It is noteworthy to mention that the stochastic theory was also studied in detailed by Gillespie (1972, 1975a, b), who derived an evolution equation for the probability mass function for the number of droplets under the assumption of no correlations. This problem was recently revisited by Wang et al. (2006), who also derived which they called the "true stochastic collection equation" (TSCE), which is a mean field equation at the first order and contains correlations among instantaneous droplets of different sizes. The problem with this equation and similar is that the rate change of moments of order n depends on moments of order $(n+1)$, as was remarked by Marcus (1968).

In our work, we overcome this drawback by calculating the true stochastic averages directly from the solution of the master equation. The main idea is to reduce the dimensionality by restricting the state space only to those states which have a finite probability of being accessed. It turns out that this provides a considerable improvement in numerical efficiency.

ACPD
15, 12213–12240, 2015

The paper is organized as follow: in Sect. 2, the numerical algorithm is explained in detail, and numerical solutions for the sum and constant kernels with a comparison with analytical solutions are presented in Sect. 3. The numerical results for mass dependent kernels along with calculation of correlations for different droplet sizes are presented in Sect. 4. Finally, in Sect. 5 we briefly discuss the results and the possible applications of the numerical algorithm.

2 The numerical algorithm

To solve Eq. (2) by brute force, the joint probability $P(n_1, n_2, \ldots, n_N; t)$ must be discretized into a multidimensional array. The main drawback of this approach is its susceptibility to the curse of dimensionality, i.e. the exponential growth in memory and computational requirements in the number of problem dimensions.

For example, for a system with a mono-disperse initial condition $P(50, 0, 0, \ldots, 0; 0) = 1$, even considering the restriction (Eq. 4), we would be in need to define a 50 dimensional array with about 3×10^{20} elements, which is computationally prohibitive.

2.1 Calculation of all possible states

Instead of the brute force discretization of the multi-dimensional joint probability distribution, the solution for this problem lies on the generation of all possible states from an initial configuration, and the posterior calculation of the time evolution of the probability $P(\overline{n}; t)$ for each generated configuration by using the master equation. From an arbitrary initial condition $P(n_{01}, n_{02}, \ldots, n_{0N}; 0) = 1$ all possible states can be generated numerically. This can be performed by taking into account that the only allowed transitions are of the form: $\overline{n}_1^{(+)} \rightarrow \overline{n}_1$ if $i \neq j$ and $\overline{n}_2^{(+)} \rightarrow \overline{n}_2$ if $i = j$, where $\overline{n}_1^{(+)}$, $\overline{n}_1$ and $\overline{n}_2^{(+)}$, $\overline{n}_2$ are the state vectors

ACPD
15, 12213–12240, 2015

$$\overline{n}_1^{(+)} = (n_1, \ldots, n_i + 1, \ldots, n_j + 1, \ldots, n_{i+j} - 1, \ldots, n_N) \quad (5a)$$

$$\overline{n}_1 = (n_1, \ldots, n_i, \ldots, n_j, \ldots, n_{i+j}, \ldots, n_N) \quad (5b)$$

$$\overline{n}_2^{(+)} = (n_1, \ldots, n_i + 2, \ldots, n_{2i} - 1, \ldots, n_N) \quad (5c)$$

$$\overline{n}_2 = (n_1, \ldots, n_i, \ldots, n_{2i}, \ldots, n_N) \quad (5d)$$

For a system consisting of N monomers at $t = 0$, $R(N)$ states (or N dimensional vectors) can be realized, where $R(N)$ is the number of solutions in integers $\overline{n}$ of the Eq. (4) for conservation of mass. The number of possible configurations can be approximated from the equation (Hall, 1967):

$$R(N) \sim \frac{1}{4N\sqrt{3}} \exp(\pi(2N/3)^{1/2}) \quad (6)$$

Note that, although $R(N)$ increases very quickly with N (for example, $R(50) = 217\,590$ and $R(100) = 190\,569\,232$), a number of states that is manageable with an average computer is obtained (compare with the 50 dimensional array with 3×10^{20} elements required for $N = 50$). Although the formula Eq. (6) slightly overestimate the number of states, it gives estimates that can be used in order to check the performance of the algorithm. For $N = 6$, 10, 20, 30 we obtained 11, 42, 627, and 5604 with the numerical algorithm, and 13, 48, 692 and 6078 by using the formula Eq. (6). As an example, the 11 possible configurations generated from the initial state $(6,0,0,0,0,0)$ are displayed in Fig. 1.

2.2 Time evolution of the probabilities $P(\overline{n};t)$ for each state

At $t_0 = 0$, for the initial state $P(n_{01}, n_{02}, n_{03}, n_{04}, \ldots; t_0) = 1$, and the probabilities for the rest of the states are set equal to 0. The probabilities of all generated configurations

ACPD
15, 12213–12240, 2015

are updated according to the first order finite difference scheme:

$$
\begin{aligned}
P\left(\overline{n};t_0+\Delta t\right) &= P\left(\overline{n};t_0\right) \\
&+ \Delta t \sum_{i=1}^{N}\sum_{j=i+1}^{N} K(i,j)(n_i+1)(n_j+1) \\
&\times P(\ldots,n_i+1,\ldots,n_j+1,\ldots,n_{i+j}-1,\ldots;t_0) \\
&+ \Delta t \sum_{i=1}^{N} \frac{1}{2} K(i,i)(n_i+2)(n_i+1) \\
&\times P(\ldots,n_i+2,\ldots,n_{2i}-1,\ldots;t_0) \\
&- \Delta t \sum_{i=1}^{N}\sum_{j=i+1}^{N} K(i,j) n_i n_j P\left(\overline{n};t_0\right) \\
&- \Delta t \sum_{i=1}^{N} \frac{1}{2} K(i,i) n_i (n_i-1) P(\overline{n};t_0)
\end{aligned}
\tag{7}
$$

It is clear from Eq. (7) that the state probabilities $P\left(\overline{n};t_0+\Delta t\right)$ at $t=t_0+\Delta t$ will increased if the states from which transitions are allowed, have a non-zero probability at $t=t_0$ (second and third terms in the right-hand size of Eq. 6), and will decrease due to collisions of particles from the same state at $t=t_0$ (fourth and fifth terms in the right-hand side of Eq. 7) if $P(\overline{n};t_0)$ is positive. The finite difference equation for $P(1,0,0,0,1,0)$ was written to illustrate the method. As can be checked from the generation scheme displayed in Fig. 1, the only allowed transitions to $(1,0,0,0,1,0)$ are from the states $(1,1,1,0,0,0)$ and $(2,0,0,1,0,0)$. Consequently, at $t=t_0+\Delta t$, $P(0,1,0,1,0,0;t_0+\Delta t)$ will increase if $P(1,1,1,0,0,0;t_0)$ and $P(2,0,0,1,0,0;t_0)$ are positive at $t=t_0$. On the other hand, $P(1,0,0,0,1,0;t_0+\Delta t)$ will decrease due to collisions from particles within the same state at $t=t_0$ if $P(1,0,0,0,1,0;t_0)$ is positive.

ACPD
15, 12213–12240, 2015

Then, $P(1,0,0,0,1,0;t_0+\Delta t)$ is calculated from the equation:

$$\begin{aligned}P(1,0,0,0,0,1,0;t_0+\Delta t) = {} & P(1,0,0,0,0,1,0;t_0)\\ & + \Delta t K(2,3)(n_2+1)(n_3+1)P(1,1,1,0,0,0;t_0)\\ & + \Delta t K(1,4)(n_1+1)(n_4+1)P(2,0,0,1,0,0;t_0)\\ & - \Delta t K(1,5)(n_1)(n_5)P(1,0,0,0,1,0;t_0)\end{aligned} \quad (8)$$

In the second term of the right-hand side of Eq. (8), n_2+1 and n_3+1 are set equal to 1, as they are the number of particles in the second and third bins in the configuration $(1,1,1,0,0,0)$ at $t=t_0$. In the third term, $n_1+1=2$ and $n_4+1=1$ as they are defined from the state $(2,0,0,1,0,0)$, and finally $n_1=n_5=1$ in the fourth and last term. As an exercise, the time evolution of each state probability was calculated for the coalescence kernel $K(i,j)=(i^{1/2}+j^{1/2})/40$ from Marcus (1968). The results for 5 of the 11 possible configurations are displayed in Fig. 2.

2.3 Calculation of the expected values of the number of particles for each particle mass

The number of particles for a given mass n_1, n_2, ..., n_N are discrete random variables whose probability distributions can be obtained from:

$$P(n,m;t) = \sum_{\text{Except } n_m} P(n_1,n_2,\ldots,n_m=n,\ldots,n_N;t) \quad (9)$$

Usually, the numerical implementation of Eq. (9) would involve calculating the sum of all elements of a multidimensional array, which is computationally very expensive. Our approach is simpler: once the probabilities of all possible states are determined for all times, $P(n,m;t)$ can be calculated just by summing over all states that have $n_m=n$:

$$P(n,m;t) = \sum_{\text{All states with } n_m=n} P(n_1,n_2,\ldots,n_m=n,\ldots,n_N;t) \quad (10)$$

ACPD
15, 12213–12240, 2015

The expected value $\langle n_m \rangle$ for the number of particles of mass m is then calculated from the equation:

$$\langle n_m \rangle = \sum_n nP(n,m;t) \tag{11}$$

As an example, for the system from Fig. 1, the probability distribution $P(n,1;t)$ of having n particles with mass $m = 1$ is displayed in Table 1.

3 Comparison with analytical solutions

The expected values for each particle mass calculated with the numerical algorithm, were tested against the analytical solutions of the master equation reported in Tanaka and Nakazawa (1993) for the constant (Eq. 12) and sum (Eq. 13) kernels ($K(i,j) = A$, $K(i,j) = B(x_i + x_j)$) obtained for the monodisperse initial condition $P(N_0,0,0,\ldots,0;0) = 1$. They are:

$$\langle n_m \rangle = C_m^{N_0} m! \sum_{l=1}^{N_0-m+1} \sum_{k=l}^{N_0} (-1)^{k-1} \frac{(2k-1)C_{l-1}^{N_0-1} C_{l-1}^{N_0-m} C_{N_0-k}^{N_0-l}}{(k+l-1)C_{k+l-1}^{N_0+k-1}} \times \left\{ (l-1) / \prod_{i=1}^{m} (N_0 - i) \right\} e^{\frac{-k(k-1)}{2}\tau} \tag{12}$$

$$\langle n_m \rangle = C_m^{N_0} \left(\frac{i}{N_0} \right)^{m-1} \left\{ 1 - \frac{m}{N_0} \left(1 - e^T \right) \right\}^{N_0-m-1} \times (1 - e^{-T})^{m-1} e^{-T} \tag{13}$$

In Eqs. (12) and (13), N_0 is the initial number of particles, $C_m^{N_0}$ is the binomial coefficient and $\langle n_m \rangle$ are the true stochastic averages for each particle mass m at time t. In Eq. (12) $\tau = AN_0t$, where $A = 1.2 \times 10^{-4}\,\mathrm{cm^3\,s^{-1}}$ is the constant collection kernel. Finally, in Eq. (13), $T = BN_0v_0t$ where v_0 is the initial volume of droplets and

ACPD
15, 12213–12240, 2015

$B = 8.82 \times 10^2\ \mathrm{cm^3\,g^{-1}\,s^{-1}}$. Turning to a concrete numerical example, the evolution of a cloud system with an initial monodisperse droplet size distribution of $N_0 = 10$ droplets of 10 µm in radius (droplet mass 4.189×10^{-9} g) at t_0, and a volume of 1 $\mathrm{cm^3}$ was calculated with the numerical algorithm. The time step was set equal to $\Delta t = 0.1$ s. A comparison between the numerical and analytical results for both the sum and constant kernels at $t = 1200$ are shown in Figs. 3 and 4 with an excellent agreement between the two approaches.

4 Kinetic vs. stochastic approach: calculation of correlation coefficients and numerical results for mass dependent collection kernels

4.1 Numerical calculation of the correlation coefficients

The evolution equation for the expected values of the random variables can be obtained by multiplying Eq. (7) by n_k and summing over all states (see Bayewitz et al., 1974):

$$\frac{\partial}{\partial t}\langle n_k\rangle = \frac{1}{2}\sum_{i+j=k} K(i,j)\left(\langle n_i n_j\rangle - \langle n_i\rangle\delta_{i,j}\right) - \sum_j K(j,n)\left(\langle n_j n_k\rangle - \langle n_j\rangle\delta_{j,k}\right) \tag{14}$$

The KCE is obtained from Eq. (14) by assuming that $\langle n_i n_j\rangle = \langle n_i\rangle\langle n_j\rangle$, i.e. that the correlation between the random variables is zero. A form of Eq. (14) was deduced in Tanaka and Nakazawa (1993) and in Wang et al. (2006) for a general type of kernels. Bayewitz et al. (1974) have quantified the deviation of the size distributions calculated with the KCE from the exact distribution obtained from the master equation for a constant kernel. From Eq. (14) it can be concluded that as long as the correlations remain appreciable, the results of the KCE will not match the true stochastic averages. The correlation (or correlation coefficient) between two random variables n_i and n_j denoted as $\rho_{i,j}$ is

ACPD
15, 12213–12240, 2015

$$\rho_{i,j} = \frac{\mathrm{cov}(n_i, n_j)}{\sqrt{\mathrm{Var}(n_i)\mathrm{Var}(n_j)}} = \frac{\sigma_{n_i n_j}}{\sigma_{n_i}\sigma_{n_j}} \tag{15}$$

In (15), the covariance ($\mathrm{cov}(n_i, n_j)$) is calculated according to

$$\mathrm{cov}(n_i, n_j) = E\left[\left(n_i - \langle n_i\rangle\right)\left(n_j - \langle n_j\rangle\right)\right] = E\left(n_i n_j\right) - \langle n_i\rangle\langle n_j\rangle \tag{16}$$

Where $E\left(n_i n_j\right)$ is the expected value of the product $n_i n_j$, which, for the bivariate case is:

$$E\left(n_i n_j\right) = \sum_{n_i}\sum_{n_j} n_i n_j f(n_i, n_j) \tag{17}$$

In Eq. (17), $f(n_i, n_j)$ is the two dimensional joint probability mas function (pmf) which was calculated similarly to how it was done in the univariate case (See Eq. 10):

$$f(n,l) = P(n,i;l,j;t) = \sum_{\substack{\text{All states with}\\ n_i = n \text{ and } n_j = l}} P(n_1, n_2, \ldots, n_i = n, \ldots, n_j = l, \ldots, n_N; t) \tag{18}$$

In the former equation, $P(n,i;l,j;t)$ is the probability of having n droplets of mass i and l droplets of mass j.

4.2 Numerical results for the constant, sum and product kernels

Correlation coefficients ($\rho_{1,2}$ and $\rho_{2,3}$) were obtained by Wang et al. (2006) using the analytical solution obtained by Bayewitz et al. (1974) for a constant collection kernel. They found that, even for this case, the magnitude of correlations could be quite large. We will extend their analysis by calculating the time evolution of the correlation coefficients $\rho_{1,2}$ and $\rho_{2,3}$ for the constant, sum and product kernels (see Fig. 5). For each

ACPD
15, 12213–12240, 2015

case, the simulations were conducted for two systems containing 10 and 40 droplets of 14 µm in radius respectively, and a volume of 1 cm^{-3}. As can be observed in the figure, in all the cases we have non-zero correlations. From the evolution of $\rho_{1,2}$ for all the kernels, we can infer that the random variables n_1 and n_2 are, at the beginning of the simulation, strongly anticorrelated. This due to the fact that in the initial stage of evolution of the system, for a monodisperse system, we have mainly collisions between size 1 droplets to form size 2 droplets. On the other hand, the random variables n_2 and n_3 are also anticorrelated, because a decrease of n_2 due to collisions with size 1 droplets will increase the number of size 3 droplets (Wang et al., 2006).

At $t = 1800$ s, the true stochastic averages (see Eq. 11) obtained numerically from the master equation are displayed in Fig. 6, together with the mean values for each droplet mass calculated from the analytical solutions of the KCE (See Table 2.). For the three cases, at the large end of the spectrum, results differ substantially. This is in agreement with the analytical of Tanaka and Nakazawa (1994), who demonstrated that the true stochastic averages coincide well with those obtained from the kinetic collection Eq. (1) if the bin mass k satisfies the inequality $k^2 \ll M_0$, where M_0 is the total mass of the system.

4.3 Numerical results for the turbulent hydrodynamic collection kernel

Collisions between droplets under pure gravity conditions are simulated with a collection kernel of the form:

$$K_g = (x_i, x_j) = \pi(r_i + r_j)^2 |V(x_i) - V(x_j)| E(r_i, r_j) \quad (19)$$

The hydrodynamic kernel (Eq. 19) does not take into account the turbulence effects and considers that droplets with different masses (x_i and x_j and corresponding radii, r_i and r_j) have different settling velocities. In Eq. (19), $E(x_i, x_j)$ are the collection efficiencies calculated according to Hall (1980). In turbulent air, the hydrodynamic kernel should be enhanced due to an increase in relative velocity between droplets (transport effect) and an increase in the collision efficiency (the drop hydrodynamic interaction).

ACPD
15, 12213–12240, 2015

These effects were taken into account by implementing the turbulence induced collision enhancement factor $P_{\text{Turb}}(x_i, x_j)$ calculated in Pinsky et al. (2008) for a cumulonimbus cloud with dissipation rate, $\varepsilon = 0.1\ \text{m}^2\,\text{s}^{-3}$ and Reynolds number, $\text{Re}_\lambda = 2\times10^4$ for cloud droplets with radii ≤ 21 µm. Then, the turbulent collection kernel has the form:

$$K_{\text{Turb}}(x_i, x_j) = P_{\text{Turb}}(x_i, x_j) K_{\text{g}}(x_i, x_j) \tag{20}$$

In the simulation for turbulent air, a system corresponding to a cloud volume of 1 cm^3 and a bidisperse droplet distribution was considered: 20 droplets of 14 µm in radius and another 10 droplets of 17.64 µm in radius, corresponding to a liquid water content (LWC) of 0.436 $\text{g}\,\text{m}^{-3}$. For the turbulent collection kernel the true stochastic averages at $t = 200$, 1800 s are displayed in Fig. 7, and compared with the mean values for each droplet mass calculated numerically from the kinetic collection equation (KCE) with kernel (Eq. 20). Also, for this case, at the large end of the spectrum, results obtained from the KCE differ substantially from the stochastic means. The time evolution of the correlation coefficients $\rho_{1,5}$ and $\rho_{1,3}$ displayed in Fig. 8 confirms the fact that correlations cannot be neglected.

Finally, the time variation of $\langle n_1 \rangle$, $\langle n_5 \rangle$, $\langle n_{15} \rangle$ and $\langle n_{20} \rangle$ were calculated and compared with the time evolution of the averages calculated from the KCE with the same initial conditions and coalescence rate. We can see from Fig. 9 that for the small masses $k = 1$ and 5, both solutions are closely coincident up to 1800 s, and that for the larger masses $k = 15$ and 20, the results are different at all times.

5 Conclusions

The full stochastic description of the growth of cloud droplets in a coalescing system is a challenging problem. For finite volume systems or in systems of small populations, statistical fluctuations become important and the mathematical description relies on the master equation which has analytical solutions for a limited number of cases. In

ACPD
15, 12213–12240, 2015

an effort to solve this problem, we have introduced a new approach to numerically calculate the solution of the coalescence multivariate master equation that works for any type of kernels and initial conditions.

For the constant, sum and product kernels, the true stochastic averages calculated numerically were compared with analytical solutions of the master equation, with an excellent agreement between the two approaches.

A numerical procedure to calculate the correlation coefficients was implemented, and we were able to calculate the correlation coefficients for mass dependent kernels (sum, product, and kernels modified by turbulent processes). Numerical solutions of the master equation for bivariate initial conditions and collection kernels modified by turbulent processes were calculated and compared with size distribution obtained from the numerical integration of the KCE. The two equations give different values at the large end of the droplet size distribution. It was also shown that, for small k, the true stochastic averages $\langle n_k \rangle$ and the solution of the KCE are closely coincident up to 1800 s. For larger masses, the results are different at all times.

The numerical algorithm reported in this paper could be very useful in order to understand the limits of applicability of the deterministic KCE. In the second part of this series, this numerical tool will be used to investigate the droplet size distribution if the collection kernel increases sufficiently rapidly with i and, and a runaway droplet is formed, also known as a gel because applications in physical chemistry (Alfonso et al., 2013). Also, further efforts will be made in order to perform simulations with a larger number of particles in the initial configuration.

Acknowledgements. The author thanks the Associate Program of the Abdus Salam International Center of Theoretical Physics (ICTP), in Trieste, Italy, where this work was started in the summer of 2013. This study was funded by grants UACM-SECITI No. PI2011-68R and Consejo Nacional de Ciencia y Tecnología de México SEP-CONACYT CB-131879.

ACPD
15, 12213–12240, 2015

References

Alfonso, L., Raga, G. B., and Baumgardner, D.: The validity of the kinetic collection equation revisited, Atmos. Chem. Phys., 8, 969–982, doi:10.5194/acp-8-969-2008, 2008.

Alfonso, L., Raga, G. B., and Baumgardner, D.: The validity of the kinetic collection equation revisited – Part 2: Simulations for the hydrodynamic kernel, Atmos. Chem. Phys., 10, 7189–7195, doi:10.5194/acp-10-7189-2010, 2010.

Alfonso, L., Raga, G. B., and Baumgardner, D.: The validity of the kinetic collection equation revisited – Part 3: Sol–gel transition under turbulent conditions, Atmos. Chem. Phys., 13, 521–529, doi:10.5194/acp-13-521-2013, 2013.

Bayewitz, M. H., Yerushalmi, J., Katz, S., and Shinnar, R.: The extent of correlations in a stochastic coalescence process, J. Atmos. Sci., 31, 1604–1614, 1974.

Gillespie, D. T.: The stochastic coalescence model for cloud droplet growth, J. Atmos. Sci., 29, 1496–1510, 1972.

Gillespie, D. T.: An exact method for numerically simulating the stochastic coalescence process in a cloud, J. Atmos. Sci., 32, 1977–1989, 1975a.

Gillespie, D. T.: Three models for the coalescence growth of cloud drops, J. Atmos. Sci., 32, 600–607, 1975b.

Hall, M. J.: Combinatorial Theory, Blaisdell Pub. Co., Waltham, MA, 1967.

Hall, W. D.: A detailed microphysical model within a two-dimensional dynamic framework: model description and preliminary results, J. Atmos. Sci., 37, 2486–2507, 1980.

Lushnikov, A. A.: Coagulation in finite systems, J. Colloid Interf. Sci., 65, 276–285, 1978.

Lushnikov, A. A.: From sol to gel exactly, Phys. Rev. Lett., 93, 198302, doi:10.1103/PhysRevLett.93.198302, 2004.

Malyshkin, L. and Goodman, J.: The timescale of runaway stochastic coagulation, Icarus, 150, 314–322, 2001.

Marcus, A. H.: Stochastic coalescence, Technometrics, 10, 133–143, 1968.

Pruppacher, H. R. and Klett, J. D.: Microphysics of clouds and precipitation, Kluwer Academic Publishers, Dordrecht, the Netherlands, 1997.

Richtmeyer, D. and Morton, K. W.: Difference Methods for Initial Value Problems, 2nd Edn., Wiley, New York, 1967.

Tanaka, H. and Nakazawa, K.: Stochastic coagulation equation and the validity of the statistical coagulation equation, J. Geomagn. Geoelectr., 45, 361–381, 1993.

ACPD
15, 12213–12240, 2015

Van Dongen, P. G. J.: Fluctuations in coagulating systems. II., J. Stat. Phys., 49, 927–975, 1987.
Van Dongen, P. G. J. and Ernst, M. H.: Fluctuations in coagulating systems, J. Stat. Phys., 49, 879–926, 1987.
Wetherill, G. W.: Comparison of analytical and physical modeling of planetesimal Accumulation, Icarus, 88, 336–354, 1990.

ACPD
15, 12213–12240, 2015

Table 1. Probability distribution $P(n,1;t)$ of finding n particles of size $m = 1$ at time t, for a system with the initial condition $P(6,0,0,0,0,0;0) = 1$.

	Probability distribution $P(n,1;t)$
$n = 0$	$P(0,1;t) = P(0,1,0,1,0,0,t) + P(0,0,2,0,0,0) + P(0,0,0,0,0,1)$
$n = 1$	$P(1,1;t) = P(1,1,1,0,0,0,t) + P(1,0,0,0,1,0)$
$n = 2$	$P(2,1;t) = P(2,2,0,0,0,0;t) + P(2,0,0,0,1,0;t)$
$n = 3$	$P(3,1;t) = P(3,0,1,0,0,0;t)$
$n = 4$	$P(4,1;t) = P(4,1,0,0,0,0;t)$
$n = 5$	$P(5,1;t) = 0$
$n = 6$	$P(6,1;t) = P(6,0,0,0,0,0;t)$

ACPD
15, 12213–12240, 2015

Table 2. Analytical size distributions of the kinetic collection equation (KCE) calculated with monodisperse initial conditions.

$K(x_i, x_j)$	$N(i,t)$	
$B(x_i + x_j)$	$N_0(1-\phi)\frac{(i\phi)^{i-1}}{\Gamma(i+1)}\exp(-i\phi)$	$\phi = 1 - \exp(-BN_0v_0t)$
$C(x_i \times x_j)$	$N_0\frac{(iT)^{i-1}}{i\Gamma(i+1)}\exp(-iT)$	$T = CN_0v_0^2t$
A	$4N_0\frac{(T)^{i-1}}{(T+2)^{i+1}}$	$T = AN_0t$

Note: Parameters β, B and C are constants, x and y are the masses of the colliding drops. N_0 is the initial concentration and v_0 is the initial volume of droplets. The index i represents the bin size.

ACPD
15, 12213–12240, 2015

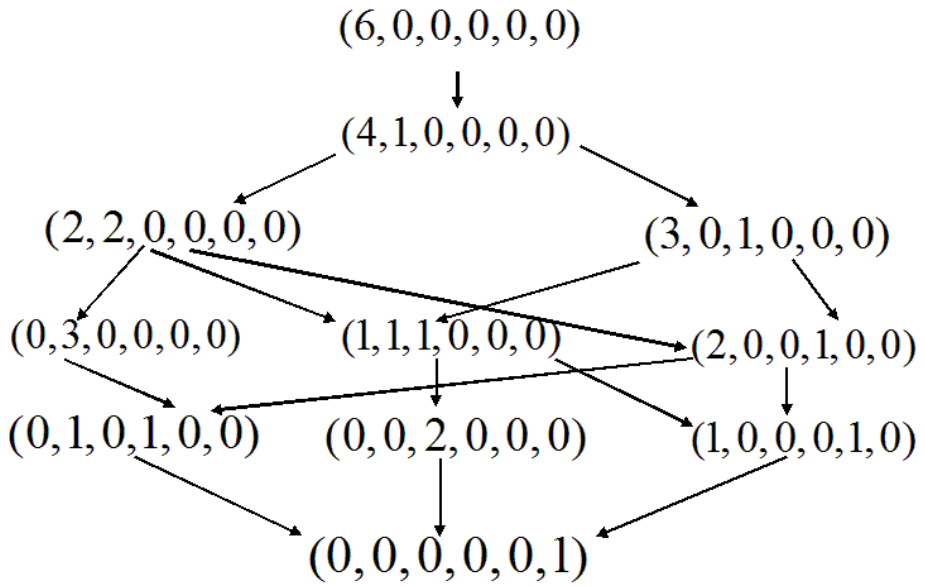

Figure 1. States space obtained from the initial condition $P(6,0,0,0,0,0;0) = 1$ with the constraint $\sum_{i=1}^{6} i n_i = 6$.

ACPD
15, 12213–12240, 2015

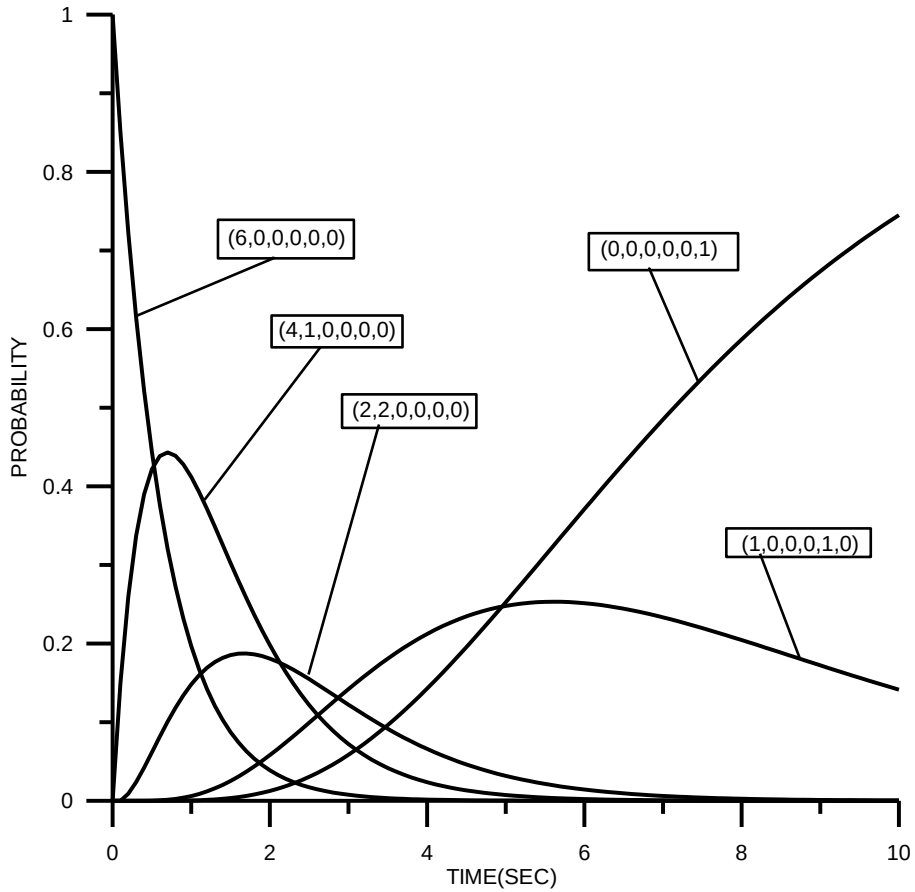

Figure 2. Time evolution of the probability for 5 of the 11 the states for the initial condition $P(6,0,0,0,0,0;0) = 1$ and the collection kernel $K(i,j) = (i^{1/2} + j^{1/2})/40$.

ACPD
15, 12213–12240, 2015

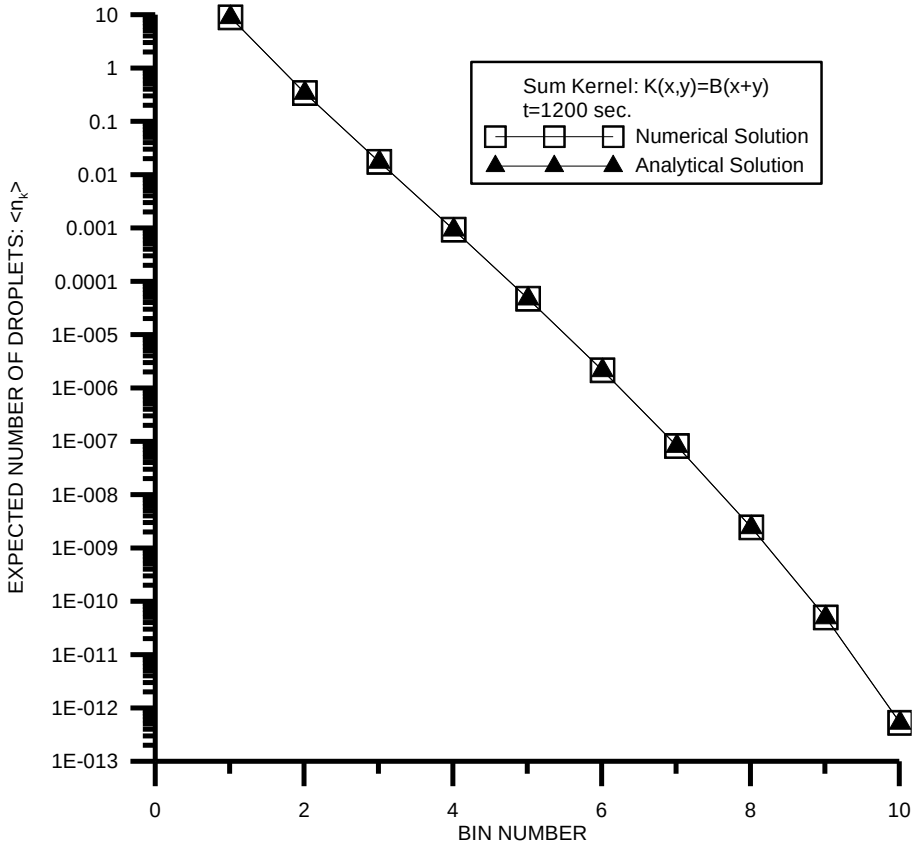

Figure 3. For the sum kernel, size distribution obtained from the analytical solution of the master equation (triangles) and the numerical algorithm (squares) at $t = 1200$ s. Calculations were performed with the initial condition $P(10,0,0,\ldots,0;0) = 1$ and the sum kernel $K(i,j) = B(x_i + x_j)$, with $B = 8.82 \times 10^2$ cm^3 s^{-1}.

ACPD
15, 12213–12240, 2015

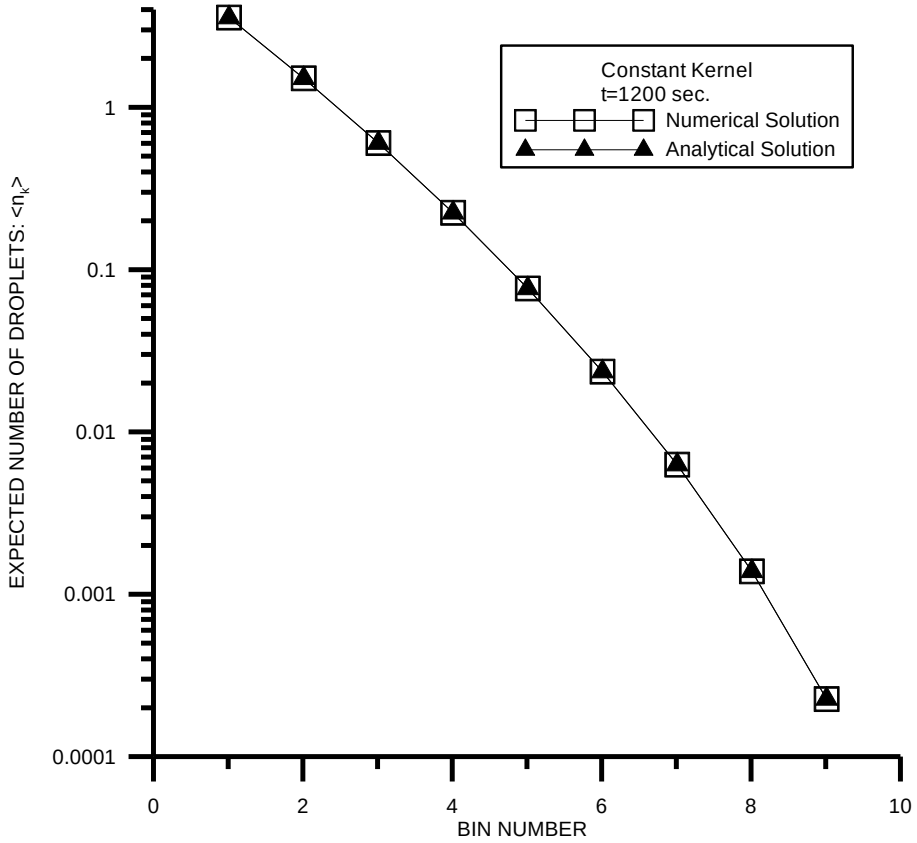

Figure 4. Same as Fig. 3 but for the constant kernel $K(i,j) = 1.2 \times 10^{-4}$ cm^{-3}.

ACPD
15, 12213–12240, 2015

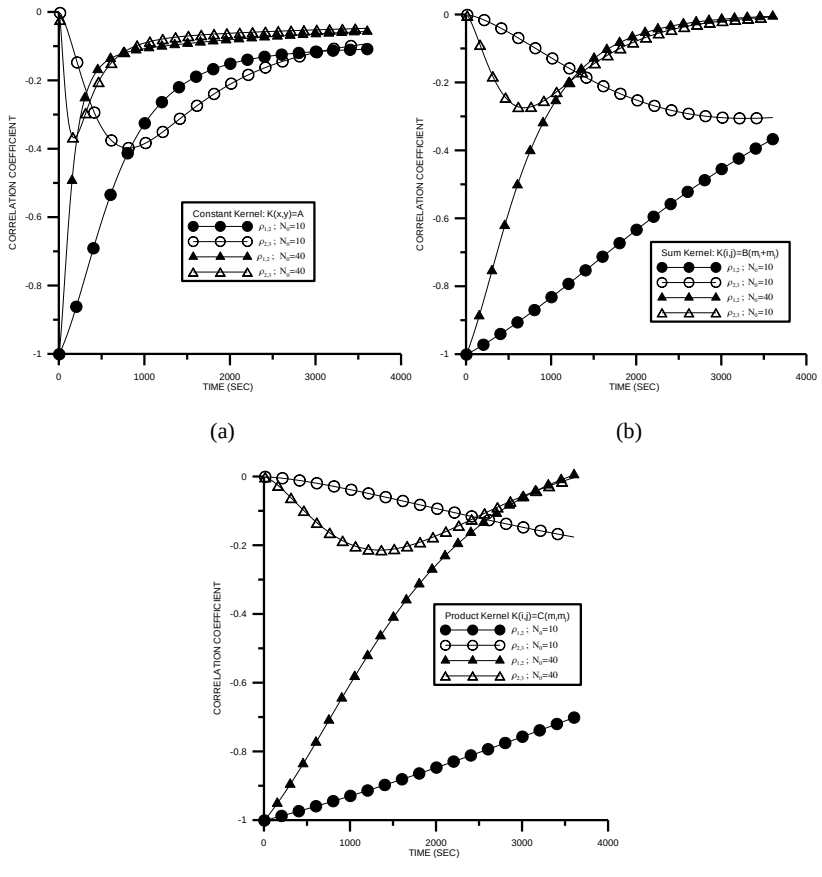

Figure 5. Time evolution of the correlation coefficients $\rho_{1,2}$ and $\rho_{2,3}$ for the constant, sum and product kernels (in **a**, **b** and **c** respectively) for two systems with a volume of 1 cm^{-3} and containing 10 and 40 droplets of 14 µm.

ACPD
15, 12213–12240, 2015

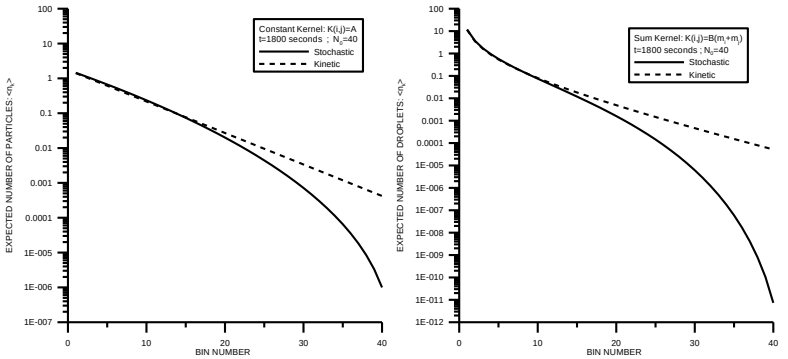

(a) (b)

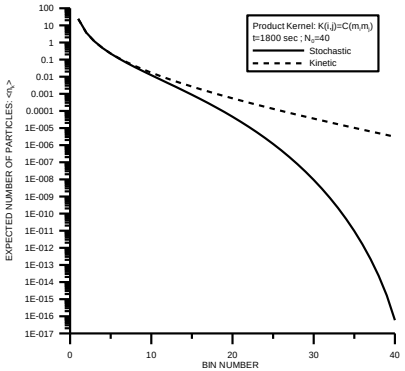

(c)

Figure 6. Comparison of the size distributions obtained from the stochastic master equation (solid line) with that to the KCE (dashed line) at t = 1800 s for a 1 cm^3 system containing initially 40 droplets of 14 µm. The expectation values are shown for the constant, sum and product kernels (in **a**, **b** and **c** respectively). For the small end the size distributions are closely coincident, for the large end the two equations give different values.

ACPD
15, 12213–12240, 2015

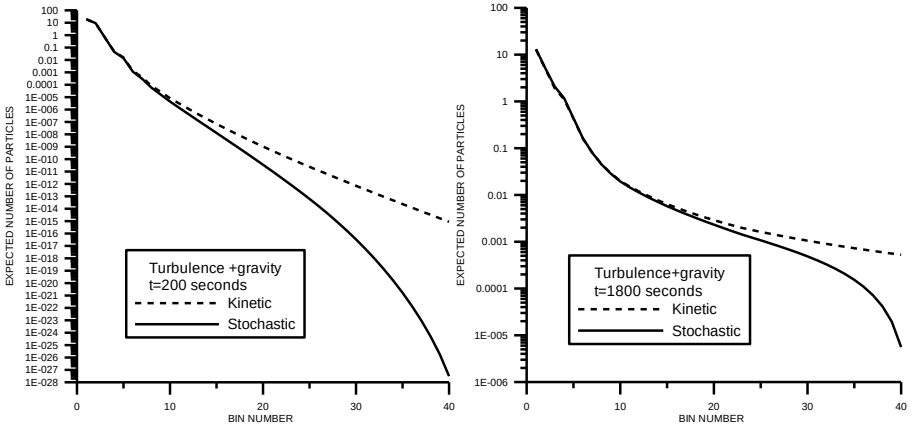

Figure 7. For the turbulent hydrodynamic kernel, comparison of the size distributions obtained from the stochastic master equation (solid line) with that to the KCE (dashed line) at $t = 200$, 1800 s for a 1 cm^3 system containing initially 20 droplets of 14 µm and 10 droplets of 17 µm. For the small end the size distributions are closely coincident, for the large end the two equations give different values.

ACPD
15, 12213–12240, 2015

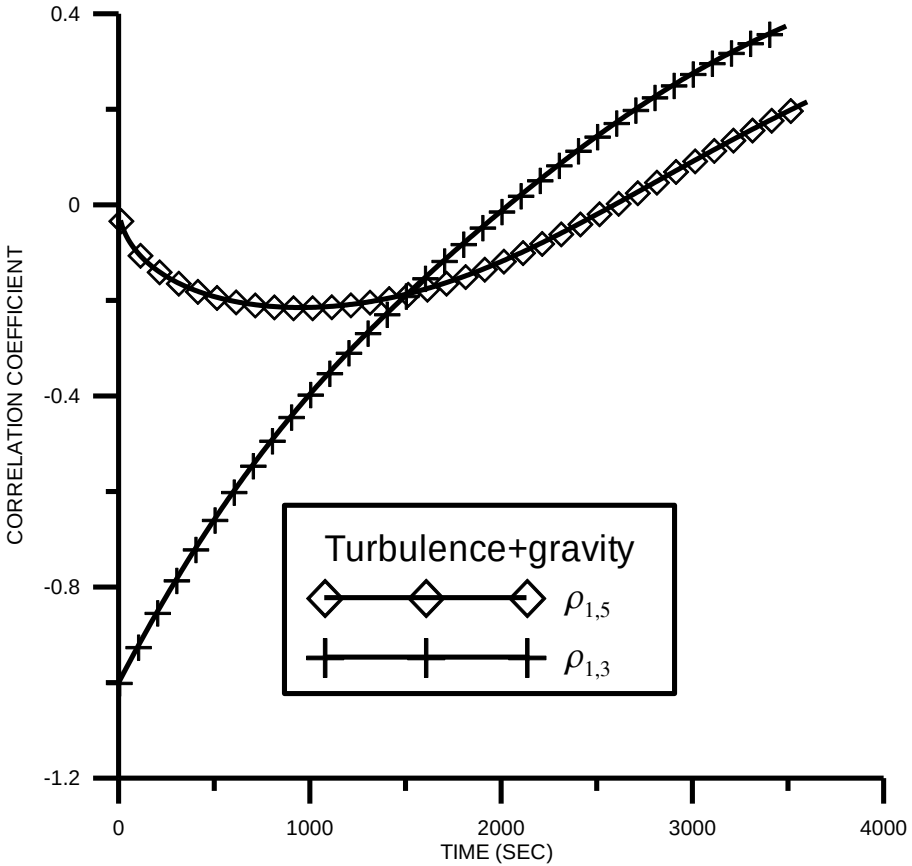

Figure 8. Time evolution of the correlation coefficients $\rho_{1,3}$ and $\rho_{1,5}$ for a 1 cm^3 system modeled with the turbulent hydrodynamic kernel and containing initially 20 droplets of 14 µm and 10 droplets of 17 µm.

ACPD
15, 12213–12240, 2015

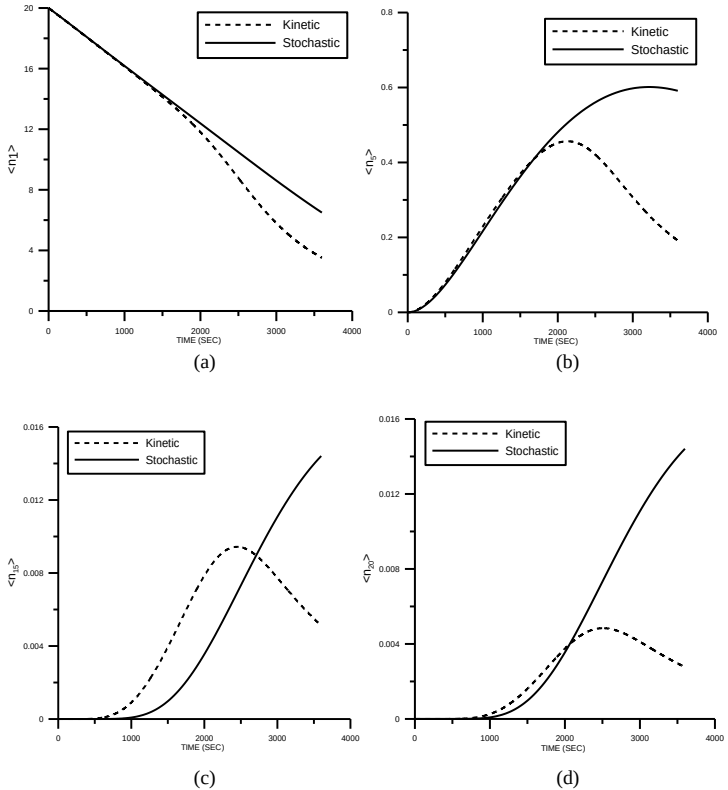

Figure 9. For the turbulent hydrodynamic kernel, comparison of the expected values obtained from the stochastic master equation (solid line) with that to the KCE (dashed line), for a 1 cm^3 system containing initially 20 droplets of 14 µm and 10 droplets of 17 µm. The time evolution of the expected values are shown for k = 1, 5, 15 and 20 (**a**, **b**, **c** and **d** respectively). For the small masses k = 1 and 5, both solutions are closely coincident up to 1800 s. For the larger masses k = 15 and 20, the results are different at all times.

ACPD
15, 12213–12240, 2015